A Robust Algorithm for Classification and Rejection of NLOS Signals in Narrowband Ultrasonic Localisation Systems

Sebastian Haigh, Janusz Kulon, *Senior Member, IEEE,* Adam Partlow, Paul Rogers, and Colin Gibson

Abstract

This paper develops a novel algorithm for classifying and rejecting non-line of sight ultrasonic signals for use in indoor positioning and measurement systems. The algorithm consists of two parts, an initial probability estimate based upon signal amplitude followed by an iteratively reweighed least squares regression that utilises the probabilities in the weight update step. This method allows for reflections to be identified and rejected while simultaneously calculating the position of a receiving node. The algorithm has been tested on data collected during experiments designed to generate many challenging specular reflections. The experiments were conducted with transducers in a variety of different positions and amplitude modulated ultrasonic signals were used with four different envelopes. The algorithm was capable of correctly classifying over 96% of narrowband signals with severe multipath effect at low computational cost.

I. Introduction

Narrowband acoustic methods have many advantages, including low cost and availability of the transducers, that make them an attractive choice for indoor positioning and localisation systems. Such systems often use time division multiplexing (TDM) techniques, i.e.: share the whole available bandwidth among the multiple transmitters at different time slots to achieve the indoor localisation. However, these methods also have significant disadvantages that make the challenge of creating robust positioning algorithms non trivial. Among these disadvantages are the presence of signals at the receiving node produced by specular reflections of previously transmitted pulses and, due to bandwidth limitations, such systems cannot rely on spread spectrum techniques often used to overcome multipath effects in systems with broadband transducers.

An example of this situation is illustrated in Fig. 1. In specular reflection, no scattering occurs and there is great similarity between the direct and reflected signals. This is useful in applications that use reflected signals such as the pulse-echo systems described in [1]. However, reflections can confuse localisation algorithms that are attempting to synthesise a 2D or 3D position from 1D range measurements. In such 2D and 3D systems, a number of beacons in known locations transmit ultrasonic bursts of short duration at time fixed intervals. The time at which each beacon begins its transmission is staggered in such a way that the burst from each beacon has time to travel to the receiver before the next beacon begins its transmission. The problems that reflections cause for these systems are highlighted in Fig. 1 and Fig. 2, namely that the receiver ends up receiving more signals than were actually transmitted.

Fig. 2 shows a typical time series representation of the data from the receiver, after the application of a single pole recursive high pass filter and a Hilbert transform to extract the signal envelope. In this figure the grey bars represent the duration of the output signal from each of the transducers. The times marked as $t_1, t_2, \cdots, t_7$ in Fig. 2 are the time to peak values of

S. Haigh and J. Kulon are with the Faculty of Computing, Engineering and Science, University of South Wales, Pontypridd, CF37 1DL, UK. e-mail: {sebastian.haigh, j.kulon}@southwales.ac.uk

A. Partlow, P. Rogers and C. Gibson are with the Rehabilitation Engineering Unit, Artificial Limb and Appliance Service, Cardiff & Vale University Health Board, Treforest, CF37 5TF, UK

This work was part-funded by the Welsh Government's ESF-funded Knowledge Economy Skill Scholarships (Grant MAXI 20422), with Cardiff and Vale University Health Board's Rehabilitation Engineering Unit and Computing and Digital Economy Research Institute of the University of South Wales

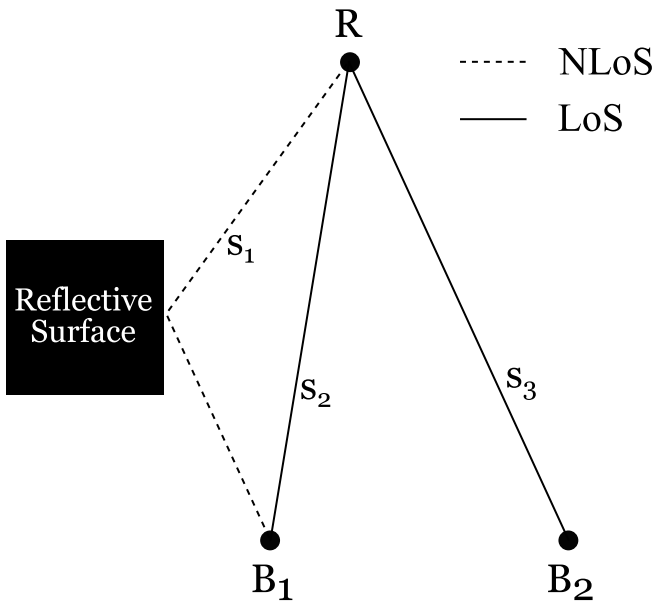

Fig. 1. Combination of Direct LOS Signals and NLOS/Multipath Propagation of Ultrasonic Signals Arriving at the Receiver (B_1, B_2: Beacon/Transmitters, R: Receiver, s_1, s_2, s_3: Three signals that arrive at the receiver.)

each of the detected signals, from which the time of flight (TOF) can be estimated, the signals marked as t_1, t_2, t_4, and t_7 are the LOS signals, the others are NLOS. There are many methods of estimating TOF of the signals such as those presented in [2]-[5]. These techniques have differing accuracy and are intended for a range of different applications, from the large scale systems with errors in the range of 0.5 metres to 1.5 metres to far more precise systems reporting submillimeter accuracy in [5]. However, when the LOS is weaker than some reflected signals, or arrives later than NLOS all conventional techniques clearly fail. The blocks in Fig. 2 are defined as the periods of time between signal transmissions. Thus the k^{th} block is the time between the start of output from beacon and the start of output from beacon $k+1$.

A. State of the Art

Methods for dealing with ultrasonic reflections have been developed and presented in the literature. These methods can, broadly speaking, be split into two main categories: least squares regression based techniques and machine learning based techniques. An example of the latter is discussed for completeness of the review, however, more focus is given to the regression based methods since the proposed technique is developed from them.

An example of a machine learning based technique is presented in [6]. This method is based upon a Support Vector Machine classifier, inspired by a similar procedure used in the Cricket localisation support system outlined in [7]. The Cricket system uses a combination of RF signals and ultrasonic signals to compute the time of flight between unsynchronised transmitters and receivers, this uses randomised signal timing along with basic statistical algorithms to overcome the effects of reflections. The filter given by [6] is reported to have an accuracy of 80% in correctly classifying LOS and NLOS signals, however this system assumes the presence of an inertial measurement unit (IMU) on-board the mobile node. The ability to exploit inertial navigation techniques to compensate for incorrect measurements allows for the accuracy of the overall localisation to be maintained by supplementing the data provided by the range measurements with data from the IMU. The system presented in [6] is designed

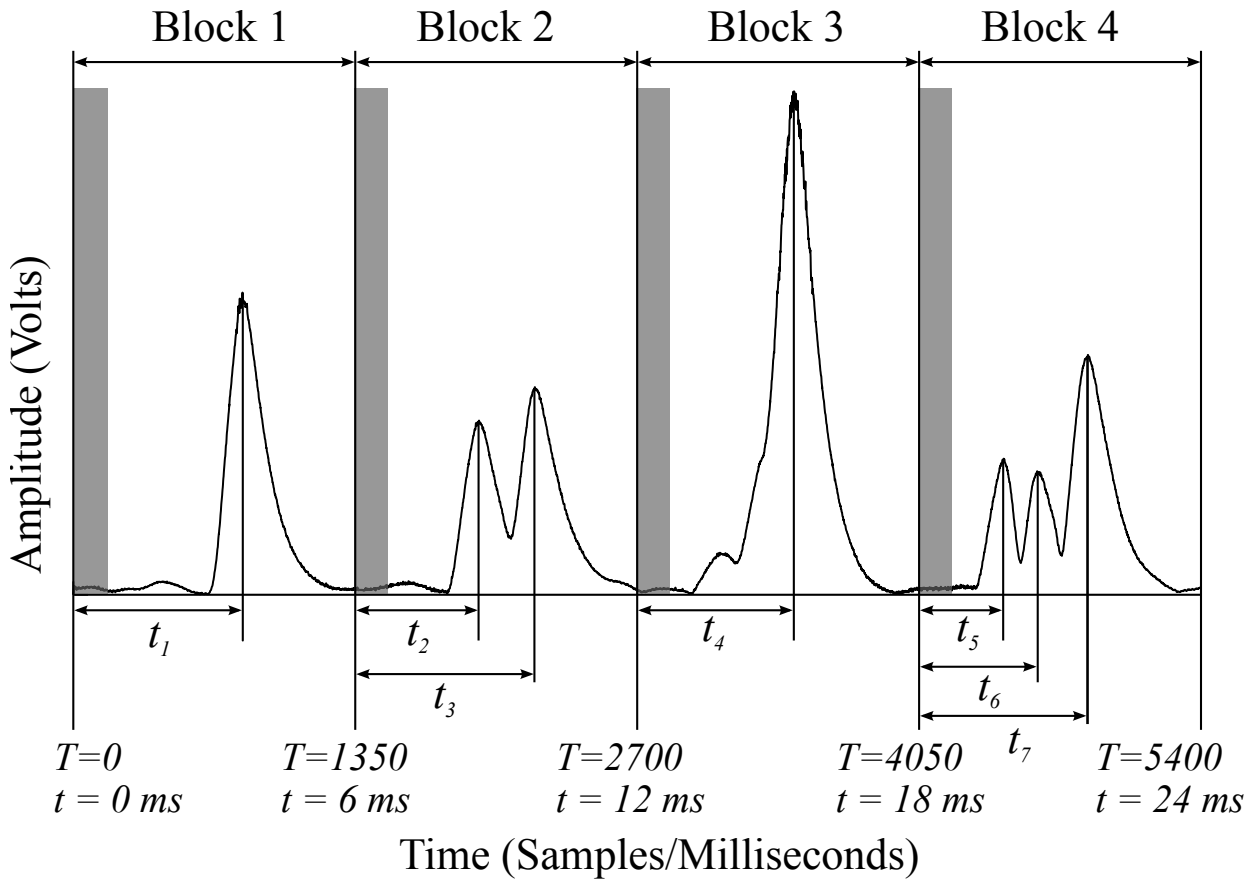

Fig. 2. A typical input from an ultrasonic sensor over a single output cycle of four transmitters featuring multiple reflections. Data has been processed by low pass filtering and envelope extraction using a Hilbert Transform. Time to peak values are indicated as well as the duration of the output signals (grey bars), block lengths are 1350 samples at 225 kHz

for use over much larger distances, as it is intended for tracking target locations within rooms. Recently Aguilera et. al. [8] proposed a multipath compensation algorithm (MCA) based on the estimation of the environment impulse response from which the corresponding LOS was obtained. The MCA in [8] uses a TDMA scheme with an additional encoding based on 255-bit Kasami sequences. The MCA was able to reduce positioning errors between 80% to 95% of the measurements depending on the reflective characteristics of the environment.

A least squares approach is presented in [9]. This study focuses on detecting outliers in the multilateration calculations and negating their effect on the final solution by use of an MM-estimator, an extension of the robust M-estimator. The M is an abbreviation of Maximum Likelihood, the repetition of the M in the extended version signifies that two M-estimates are used to increase robustness. The MM-estimator is combined with a Least Trimmed Squares (LTS) method. In LTS the algorithm searches for the subset of the total data that produces the lowest least squares solution. This requires many regressions to take place, one for every subset, and is thus a fairly slow technique.

The number of regressions needed for a given number of reflections can be determined using the well known binomial coefficient.

$$\begin{pmatrix} a \\ k \end{pmatrix} = \frac{a!}{k!(a-k)!} \tag{1}$$

In equation 1, k represents the number of signals needed to calculate the position, i.e.: the size of the subset, and a is the total number of signals received. It can be seen that the number of times the regression must be performed increases greatly with the number of reflections. In a system with four transmitters and 1, 2, 3, or 4 reflections present the system would require 5, 15, 35, or 70 regressions respectively. In systems that feature more transmitters the problem only increases; 8 transmitters and 4 reflections would require 495 regressions.

While robust regression techniques perform well at the task of outlier rejection, this performance requires a significant increase in computational cost. Additional contributions to this problem are shown in [10], where a least median squares (LMedS) approach is taken, and [11] which is LTS based. Unfortunately the LMedS technique, like the LTS, uses comparisons of different subsets to work, and therefore inherits the above problem.

In order to address the problem of maintaining robustness while maximising efficiency, the authors in [10] develop a probabilistic technique to determine which of the subset combinations is most likely to be correct, thereby allowing their algorithm cut down on computation time by immediately rejecting unlikely combinations before the regression takes place. The method in [10] uses the number of multiplications required as an indicator of the computational complexity of the algorithm. The complexity quoted by that paper is: $235LK + 280M$ for 10 iterations. Where L is the number of beacons chosen per subset for the LMedS technique, M is the total number of signals received and $K = {}^{M}C_{L}$, that is all the possible combinations. With $L = 3$, $K = 56$ and, $M = 8$ as used in [10], this results in over 41,720 multiplications.

While both [10] and [11] were developed for radio frequency system, the mathematics of regression is the same as for ultrasonic signals. Our research attempts to take these techniques in a different direction. In this paper we describe a new Robust Bayesian Classifier for Ultrasonic Localisation (RoBCUL). The proposed approach uses a combination of Bayesian probability and regression techniques in a localisation system to form a novel method of detecting and rejecting reflected ultrasonic signals while simultaneously calculating the three dimensional position of the receiving node. In the method proposed here we get rid of the subset search altogether, instead of an LTS or LMS approach, an iteratively reweighted least squares (IRLS) approach is adopted. Since we are no longer searching for appropriate subsets, the probability is calculated with respect to the individual signals received.

It is envisaged that the work presented in the paper will lead to new applications of ultrasonic localisation, such as the one recently described by the authors in [12], in which robust rejection of reflected signals is an essential component.

The following sections will develop and test this strategy. Development of the RoBCUL is described in section II. Section III outlines how the proposed algorithm has been tested with experimental data, results from this testing are presented and discussed in section IV.

II. Proposed RoBCUL algorithm

The NLOS signals have similar characteristics to the LOS signals, namely the same frequency and envelope shape. An attempt was made in [6] at classifying LOS/NLOS signals based on envelope shape which gave very poor results. The similarity in envelope shape between LOS signals and NLOS signals can be easily seen in Fig. 2.

The envelope shape of reflections can change, depending on the geometry of the surface that the signal has reflected from as described in [4], however taking advantage of this fact would require detailed knowledge of the geometry of the surrounding environment. Furthermore, Fourier analysis of a signal comprised of LOS/NLOS components shows that there is no significant difference in frequency characteristics between the two and thus spectral analysis offers no information that is useful in attempting to classify them.

The signals shown in Fig. 2 also serve to demonstrate that neither amplitude of the received signals nor the order of arrival of the signals can be used alone to determine if a signal is LOS or NLOS. The NLOS signal t_3 has greater amplitude than LOS signal t_2 and the NLOS signals t_5 and t_6 arrive before LOS signal t_7. While these characteristics offer some insight, they do not provide enough information by themselves to enable a confident classification of the signals.

There are two features that are readily available for use in classifying the received signals and rejecting reflections, they are the amplitudes of received signals and the residual errors that those signals generate when used in a regression. This section develops a RoBCUL algorithm that uses these features to reject reflected signals.

A. Bayesian Classification

The goal of classification is to determine which of a particular set of classes an object of interest belongs to. We can define a signal's membership in a particular class as $\phi \in \{0, 1\}$ where $\phi = 1$ if the signal is LOS and $\phi = 0$ otherwise. An estimate, $\hat{\phi}$, can be achieved using Bayesian techniques. Such methods are used in a wide variety of applications and a good general overview of such techniques is given in [13]-[15].

Amplitude has been chosen as a suitable feature for this step based on the assumption that a multipath NLOS signal would have travelled further than a LOS signal, thus the amplitude should be diminished due to attenuation. However, this cannot be guaranteed, and there are instances in which NLOS signals have a greater amplitude than LOS signals, therefore, classifying such signals based on their amplitude alone is ambiguous. Due to this ambiguity, instead of directly classifying signals based on their amplitude we use a Bayesian hypothesis test and normalisation step to calculate probabilities that can later be used as weights in a regression step.

Let A be the event that the signal is LOS based on amplitude, let A^* be the event that the signal is NLOS. With s_i denoting the measured amplitude of the i^{th} received signal, the hypothesis test can be given as in equation 2. Where the likelihoods $p(s_i|A)$ and $p(s_i|A^*)$ are the probabilities that the signal i is LOS and NLOS respectively.

$$\hat{\phi}^-_{b_k|s_i} = p(A|s_i) = \frac{p(s_i|A)p(A)}{p(s_i|A)p(A) + p(s_i|A^*)p(A^*)} \tag{2}$$

The notation $\hat{\phi}^-_{b_k|s_i}$ denotes the probability calculated for the i^{th} signal in the k^{th} block. The superscript $-$ denotes that this probability is prior to the normalisation step, which is given by equation 3. This is used to ensure that all of the probabilities in each block sum to one.

$$\hat{\phi}_{b_k|s_i} = \frac{\hat{\phi}^-_{b_k|s_i} p(s_i)}{\sum_{j=1}^{n} \hat{\phi}^-_{b_k|s_j} p(s_j)} \tag{3}$$

The result, after this step, is a probability assigned to each signal in each block, based upon each signal's own amplitude and how its amplitude relates to the other signals in the block.

The likelihoods $p(s_i|A)$ and $p(s_i|A^*)$ in equation 2 are calculated from a pair of Gaussian probability density functions that attempt to model the distribution of LOS and NLOS amplitudes. This calculation is performed by numerically integrating each of the destiny functions over a small interval around the amplitude of the signal. Here the region used was the interval $(s_i - 0.02, s_i + 0.02)$.

The mean and standard deviations of the probability density functions were generated by a combination of statistical analysis and some experience in dealing with the system. A random sample of experimental data was selected in which it was explicitly known which signals were LOS and NLOS. The amplitudes of each signal in each of the two categories were recorded and the means and standard deviations extracted.

Due to the shape of the Gaussian density function, if the mean is a positive value then there is part of the function that will return lower probabilities for amplitudes that are lower than the mean. Since this is not an effect that is desirable for this situation, after a process of trial and error it was found that better results could be achieved by setting the mean of the pdf for NLOS signals to zero and the standard deviations of each of the functions equal, thereby guaranteeing that the highest NLOS probabilities are generated by the signals with lowest amplitudes.

$p(A)$ is provided by a uniform probability mass function generated from the number of signals in the block. $p(A^*)$ is then the sum of the probability masses of everything that is not $p(A)$. For example, if there are three signals, the uniform distribution will give, for each signal, $p(A) = 1/3$ and $p(A^*) = 2/3$, for two signals the priors would both be equal to one half.

B. Levenberg-Marquardt Method for Minimising the Objective Function

In order to minimise the objective function given in equation 4 the RoBCUL uses the Levenberg-Marquardt (LM) algorithm. First developed in [16] this method has been used in a wide range of regression applications, including acting as the base algorithm for the work presented in [9].

$$f(\mathbf{x}) = \frac{1}{2}\sum_{j=1}^{m} r_j^2(\mathbf{x}) \tag{4}$$

The vector $\mathbf{x} = [\hat{x}, \hat{y}, \hat{z}]^T$ holds the current estimate of the receiver coordinates. The residual vector $r(\mathbf{x})$ is shown in equation 5, where d_k is the measured distance between the receiver the k^{th} transmitter, and x_k, y_k, z_k are the known coordinates of that transmitter. The residuals, therefore, are the difference between the measured distance and the distance calculated using Euclidean geometry and the current estimate of the parameters.

$$r_k(\mathbf{x}) = d_k - \sqrt{(\hat{x} - x_k)^2 + (\hat{y} - y_k)^2 + (\hat{z} - z_k)^2} \tag{5}$$

The Levenberg-Marquardt method serves as the base algorithm for the IRLS. The LM algorithm with weighting is given by equation 6, where $\mathbf{W}$ is a weight matrix, $\mathbf{J}$ is the Jacobian matrix of the function $f(\mathbf{x})$, and $\mathbf{J}^T\mathbf{J}$ is an valid approximation to

the Hessian matrix where, for each cell in the Hessian either the residual is very small or the function is near linear close to solution.

$$\mathbf{x}_{i+1} = \mathbf{x}_i - \left(\mathbf{J}^T\mathbf{W}\mathbf{J} + \lambda \text{diag}\left(\mathbf{J}^T\mathbf{W}\mathbf{J}\right)\right)^{-1}\mathbf{J}^T\mathbf{W}r(\mathbf{x}) \tag{6}$$

The use of the Levenberg-Marquardt algorithm allows for a more liberal approach to the signals that are sent to the regression, and also for a more relaxed constraint on the selection of the initial starting parameters than would be the case for the Gauss-Newton algorithm on which it is based.

C. Iteratively Reweighted Least Squares

The regression is, in effect, being used as a classifier. To enable this an iteratively reweighted least squares (IRLS) method is used, with the update rule for the weights at each step taking into account the probabilities calculated earlier and the residual calculated in during the regression.

Firstly, a weight matrix is required. This will be initially populated with the probabilities calculated from the amplitudes of the signals.

The subscript $k|i = \text{block}|\text{signal}$ notation used in the probability step will be maintained here. $w_{k|i}$ is the weight of the i^{th} signal in the k^{th} block, while the block number may be different these are all, of course, part of the same matrix.

$$W = \begin{bmatrix} \hat{\phi}_{k=1|i=1} & 0 & \cdots & 0 \\ 0 & \hat{\phi}_{k=1|i=2} & & \vdots \\ \vdots & & \ddots & 0 \\ 0 & \cdots & & \hat{\phi}_{k=N_b|i=N_s} \end{bmatrix} \tag{7}$$

The initial weight matrix is shown in equation 7, where N_b is the number of blocks, and N_s is the number of signals in block $k = N_b$. Thus the probabilities are arranged in the order that their respective signals appear in the given frame. The update rule for the weights, defined with respect to a constant threshold value γ is given as:

$$w_{k|i} = \begin{cases} \frac{\gamma}{|r_{k|i}|}\hat{\phi}_{k|i} & \text{if} \quad |r_{k|i}| > \gamma \\ \\ 1 & \text{else} \end{cases} \tag{8}$$

The weight, updated in this way, allows for the probability calculated earlier to push the solution in the most probable direction, using a combination of probability based on amplitude and regression residual. The constant γ should be a small value in the expected range of error for the line of sight signals in the system. However, if the value is too small compared to the accuracy then the residual of a LOS signal may never reach the value, if it is too large then NLOS signals may have residuals less than it.

This system can take a long time to converge, in order to speed up the process a second weight update is implemented. The value of the individual weights can be further manipulated by taking into account the value of each residual compared to the other residuals of the same block.

Due to the timing of the transmitted signals we know that only one of the signals in each block can be the LOS signal. This information can be leveraged to reach the result faster while minimising the negative effects this may have on the algorithm making an incorrect classification. This works by detecting the minimum residual in each block (for blocks with more than one signal) and increasing the respective signals weight by multiplying it by a constant factor $q > 1$. The signal with the lowest residual is detected by the first part of equation 9. This signal then receives a slight boost in its weight, however, this boost is just a nudge in the right direction and is relatively small compared to the main re-weighing step shown in equation 8.

$$\begin{aligned} j &= \text{argmin}\{r_{k|i=1}, r_{k|i=2}, \cdots, r_{k|i=N_s}\} \\ w_{k|j}^{n+1} &= w_{k|j}^{n} q \end{aligned} \tag{9}$$

If $w_{k|j}^{n+1} > 1$, then this weight will be set to 1 before continuing. q itself is a constant value, and similar to γ, it also has a range of effective values. If it is too small it won't have any effect, and if it is too large it will cause the algorithm to become unstable. This study has found, through experiment, that $q = 2$ has a good effect in speeding up convergence without effecting stability.

D. Final Classification

Classification of the signals can be performed after convergence is achieved by classifying the signal in each block with the highest weight as the LOS signal. After this classification the regression can be continued as a standard regression with the NLOS signals removed.

This is done because some LOS signals may not have been fully weighted while some NLOS signals may still have a low, but non-zero, weight. These factors will effect the result of the regression if they are left in.

Attempts to further force the weights in either direction, down in the case of NLOS signals or up in the case of LOS signals, can have undesirable side effects, namely reducing the stability of the algorithm and causing divergence.

Utilising a hard classification at this point, and completely rejecting the signals currently classified as NLOS, ensures that there is no undue influence of either NLOS signals with non-zero weight or LOS signals with a weight less than one.

The progress made by the algorithm while classifying the signals need not be lost, and when the algorithm is restarted it can begin at the last estimate of the parameters that were calculated before the hard classification was performed. Furthermore, because the only signals left will be the LOS signals and the parameter estimates will already be close to the true solutions, the regression can be continued with a pure Gauss Newton method without need for the additional complexity of the Levenberg-Marquardt algorithm.

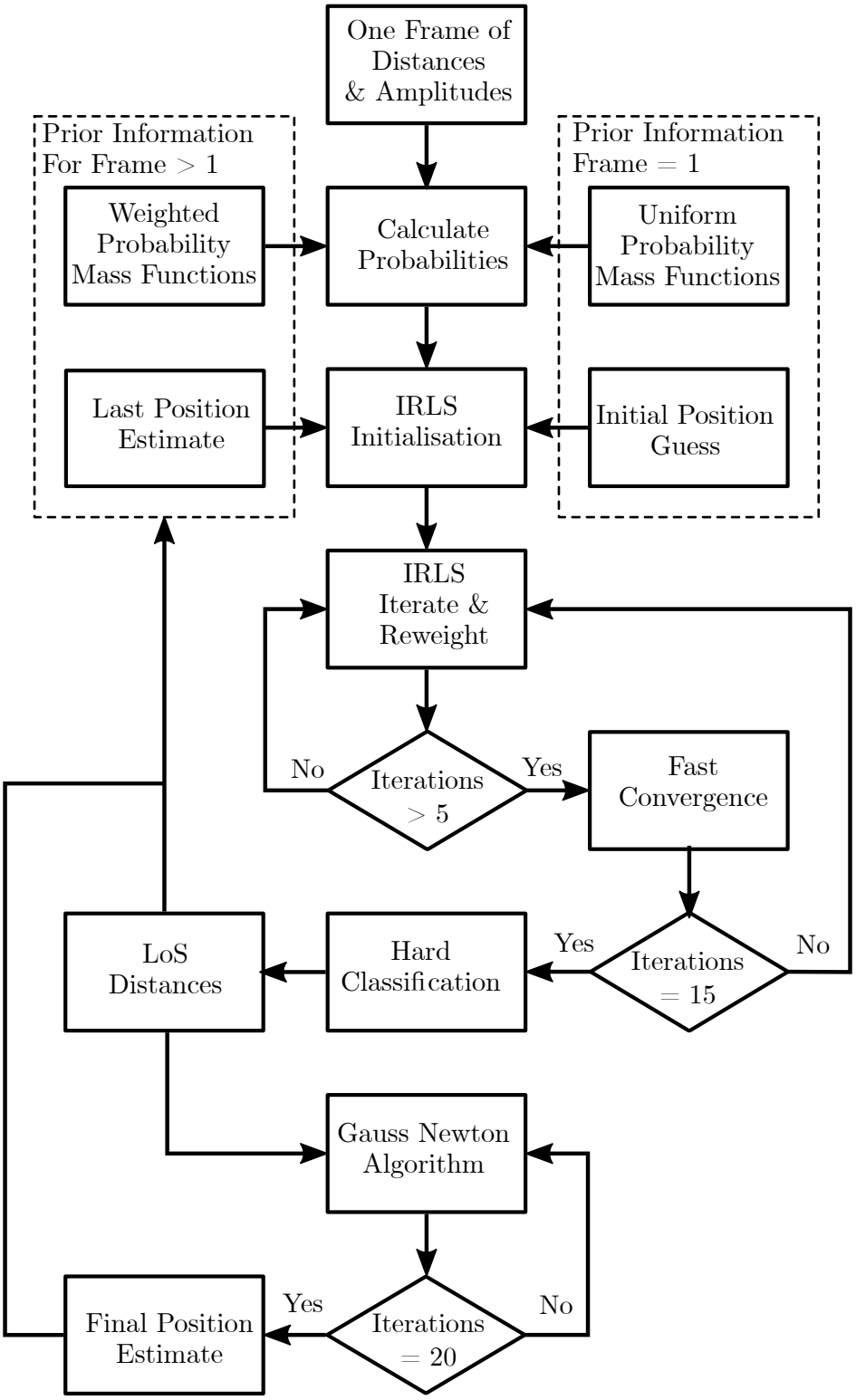

Fig. 3. Flowchart of the RoBCUL Algorithm

E. RoBCUL Summary

The flowchart of the RoBCUL is shown in Fig. 3. The algorithm consists of two main parts: first, Bayesian probability assignment for the LOS and NLOS signals and second, adaptive IRLS classification using a combination of probability based on

amplitude and regression residual. The algorithm starts with the first frame of data collected, and uses a uniform distribution as prior information to calculate the probability, as well as an initial guess for the position in order to initialise the IRLS regression algorithm.

The IRLS algorithm runs, using the fast convergence rule given in equation 9 after the 5th iteration to speed up convergence. At the 15th iteration a hard classification is performed. The signals with the highest weight in each block are chosen as the LOS signals, all other signals are rejected. The algorithm then proceeds using the Gauss Newton method to produce a final position estimate without any influence from NLOS signals.

Finally, the position estimate and LOS distances are passed to the next frame. The LOS distances are used to generate prior probability mass functions for each block, weighted to favour signals having similar distances to the ones previously classified as LOS. The previous position estimate is used to initialise the IRLS algorithm, as starting at the last known position allows the algorithm to converge to the new position faster.

F. Computational Complexity

The method developed in this paper uses an iteratively reweighted LM algorithm that eliminates the need for the subset searching method used in [10]. This creates a difference in the computational cost of the two algorithms. In order to eliminate the multiple regressions required by [10] the proposed method uses a Jacobian matrix with a number of rows equal to the number of signals received, i.e. a matrix of variable dimension, causing the computational cost of the matrix algebra to be dependent on the number of signals received.

We will now compare these two techniques and show that the proposed method can find solutions at a lower computational cost than the method outlined in [10]. Using a to represent the total number of received signals and p as the number of parameters to be estimated, the number of multiplications required per iteration is given in equation 10.

$$p^3 + a^2p + ap^2 + ap + a \tag{10}$$

a^2p is the number of multiplications required to multiply the transposed Jacobian by the weight matrix, and ap^2 multiplications are needed to multiply this again by the Jacobian to obtain the $\mathbf{J}^T\mathbf{W}\mathbf{J}$ Hessian approximation which will always be a $p \times p$ matrix, for which p^3 multiplications are needed to find the inverse. ap is required to multiply the already obtained $\mathbf{J}^T\mathbf{W}$ by the residual and finally a linear factor of a is required to for the probability calculations.

Since the number of parameters, x, y, z, being estimated is a constant 3 the expression in 10 can be reduced to the expression shown in equation 11.

$$3a^2 + 13a + 27 \tag{11}$$

As an example: for total of 8 and 16 received LOS and NLOS signals, this method requires 6,460 and 20,060 multiplications for 20 iterations, respectively, compared to the 41,720 for 8 signals in [10].

TABLE I
INITIAL PARAMETER VALUES

Parameter Name	Notation	Init. Val.	Unit	Const.
NLOS pdf mean	μ_{NLOS}	0	Volts	Yes
NLOS pdf std. dev.	σ_{NLOS}	0.35	Volts	Yes
LOS pdf mean	μ_{LOS}	0.71	Volts	Yes
LOS pdf std. dev.	σ_{LOS}	0.35	Volts	Yes
Initial LM Parameter	λ	1	None	No
LM Criterion	λ_C	0.001	None	Yes
LM Increment	λ_I	2	None	Yes
Weight Update Threshold	γ	0.01	Metres	Yes
Fast Convergence Factor	q	2	None	Yes
Initial Guess for x	$\hat{x}_0$	0	Metres	No
Initial Guess for y	$\hat{y}_0$	0	Metres	No
Initial Guess for z	$\hat{z}_0$	1	Metres	No

III. EXPERIMENTAL TESTING

In order to demonstrate the validity of the proposed algorithm the method has been tested on data collected during experiments. The results will be presented summarising the performance of the method across all the data available, and also for a specific case in order to illustrate the details of how the method works. The RoBCUL described in this paper has been developed in MATLAB and requires a number of parameter values to be specified before the program is used. These are constants or parameters that change every iteration, but require user specified initial values. The list of parameters and their values used in the tests is shown in Table I.

A. Experimental Set Up

The RoBCUL has been tested on data collected during a series of experiments. These experiments investigated different configurations of transmitters and receivers.

Two configurations of four transmitters were tested. Both configurations were square, planar arrangements of transmitters, one being a square with edge length 30 cm and one with edge length 50 cm, as shown in Fig. 4. The arrangement was planar in that while the x, y positions of each transmitter were varied to create the square, the z position was maintained constant.

The transmitters were held in position by inserting them through holes in a plywood board. The plywood board was itself mounted upon a support, to raise it from the ground.

The receivers were placed into a similar board, but with a more varied configuration, as shown in Fig. 4. The receiver positions had the same 30 cm and 50 cm square configuration, while also having positions on the midpoints of the lines between the square positions and one at the centre of the overall configuration. The receiver board was likewise mounted upon a support. The transmitters and receiver boards were both placed upon a rail on the ground, to ensure that the relative positions of transmitters and receivers could be easily controlled and measured.

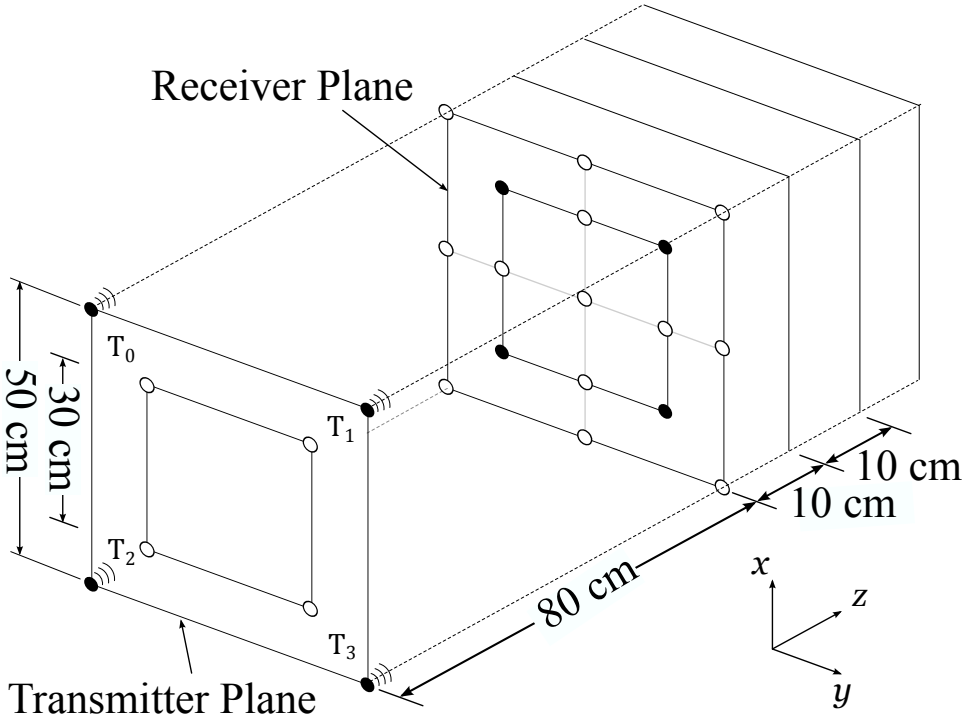

Fig. 4. Diagram of the experimental arrangement of the transducers showing: a) the transmitter plane, b) the receiver plane in initial position 80 cm from the transmitter plane, c) the incremented positions of the receiver plane. The filled circles in the diagram represent the current position of the transducers while the empty circles show different possible configurations used in the experimental test.

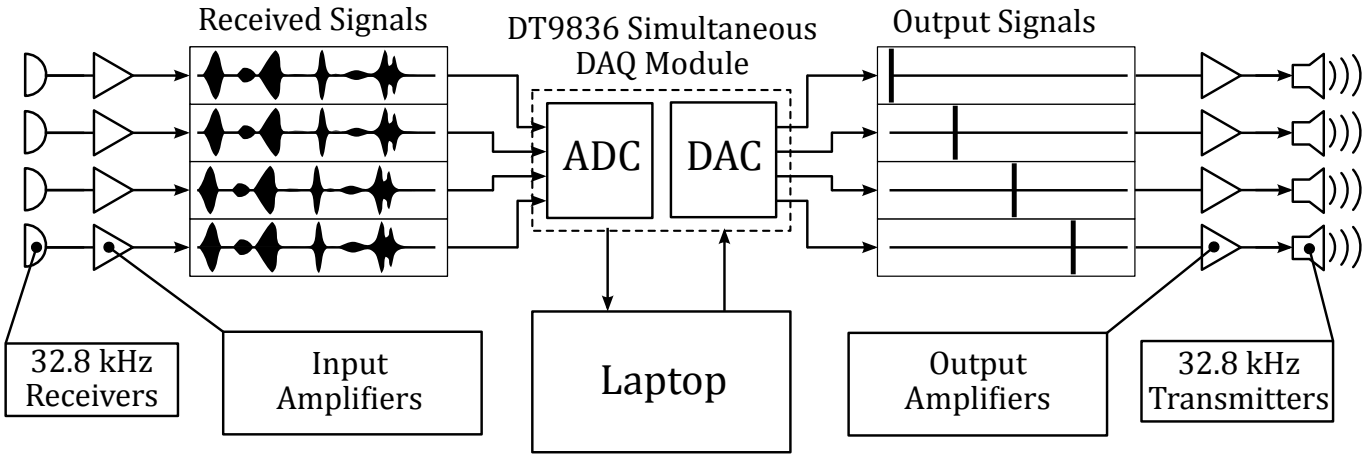

Fig. 5. The hardware components of the measurement system

Experiments were performed both with and without foam padding covering the plywood board holding the receivers. The foam padding was acoustically absorbent, helping to reduce the number of specular reflections from the highly reflective plywood surface.

The measurement system is shown in Fig. 5. The main elements of the system are: four ultrasound transmitters, four ultrasound receivers, DA/AD converter, transmitter amplifiers, programmable receiver amplifier and a laptop running a signal processing algorithm. The transmitters and receivers used in this experiment were Prowave 328ST160 and 328SR160 respectively, these transducers have a centre frequency of 32.8 kHz. The transmitters generate 115 dB SPL with 0 dB reference of 0.0002 μbar per 10 V_{RMS}, while the receivers used have a sensitivity of -67 dB with 0 dB reference of 1 V/μbar. The transmitters driving

voltage was 20 V_{RMS}. The transmitted signals were passed through a Texas Instruments THS6012 Amplifier and the received signal was conditioned using an Alligator Technologies USBPIA-S1 programmable instrumentation amplifier before being delivered to the analog-to-digital converter. The USBPIA-S1 is a standalone USB controllable module and provides a single channel of high-quality instrumentation amplifier and optional AC coupling, for front-end signal conditioning compatible with DA/AD converter. The amplifier is programmable from the USB port and provides software-selectable gain up to 1000 as well as differential inputs with high-common mode rejection.

A Data Translation DT9836 (MA 01752-1192 USA) series simultaneous DAQ module was used for output of the driving signals from MATLAB and recording the incoming signals from the receivers. DT9836 has four D/A and six A/D converters that can sample data simultaneously and continuously at maximum frequency of 225 kHz per channel for analog inputs and run at 500 kHz for each of the analog outputs. The simultaneous input and output sampling of this module allowed for the transmitters and receivers to be fully synchronised in time with the use of a hardware trigger to start all input and output channels at the same time.

B. Experimental Method

With the four transmitters in the 30 cm square configuration and the receiver board positioned 80 cm from the transmitter board a train of signals were set from each of the transmitters for a duration of 1 second. The data from each of the four receivers was recorded into MATLAB simultaneously.

Four different single frequency amplitude modulated signals were tested: square, trapezoid, triangle and sawtooth envelopes. Plots of the output signals are shown in Fig. 6, the amplitude has been normalised. Once this process was completed, and the data saved, the four receivers were placed into a different configuration and the above process was repeated. This was done until each position on the receiver board has had a receiver for at least one of the runs. The receiver board was moved 10 cm away from the transmitter board and the above process was repeated. This procedure was performed for each of 80, 90, 100, 110, 120 and 130 cm distances between the two boards. The receivers were positioned into the 50 cm square configuration and the whole process was repeated with the transmitters in these positions.

IV. Results and Discussion

The following section discusses the results from testing the developed algorithm on data collected from the experiments. Results are presented from a specific example, to demonstrate the working of the algorithm as well as general results for the entire dataset to illustrate the performance of the method in classification of NLOS signals.

A. Fast Convergence

Fig. 7a to 7d show the residuals of each of the signals from the frame previously presented in Fig. 2. In these figures dashed lines are LOS signals while the solid black lines are the reflected NLOS signals.

Analysing the residuals of the signals by block gives an insight into how the algorithm works. Firstly, it can be seen that for those blocks that contain only one signal as shown in Fig. 7a and 7c, the residual converges very quickly to near zero.

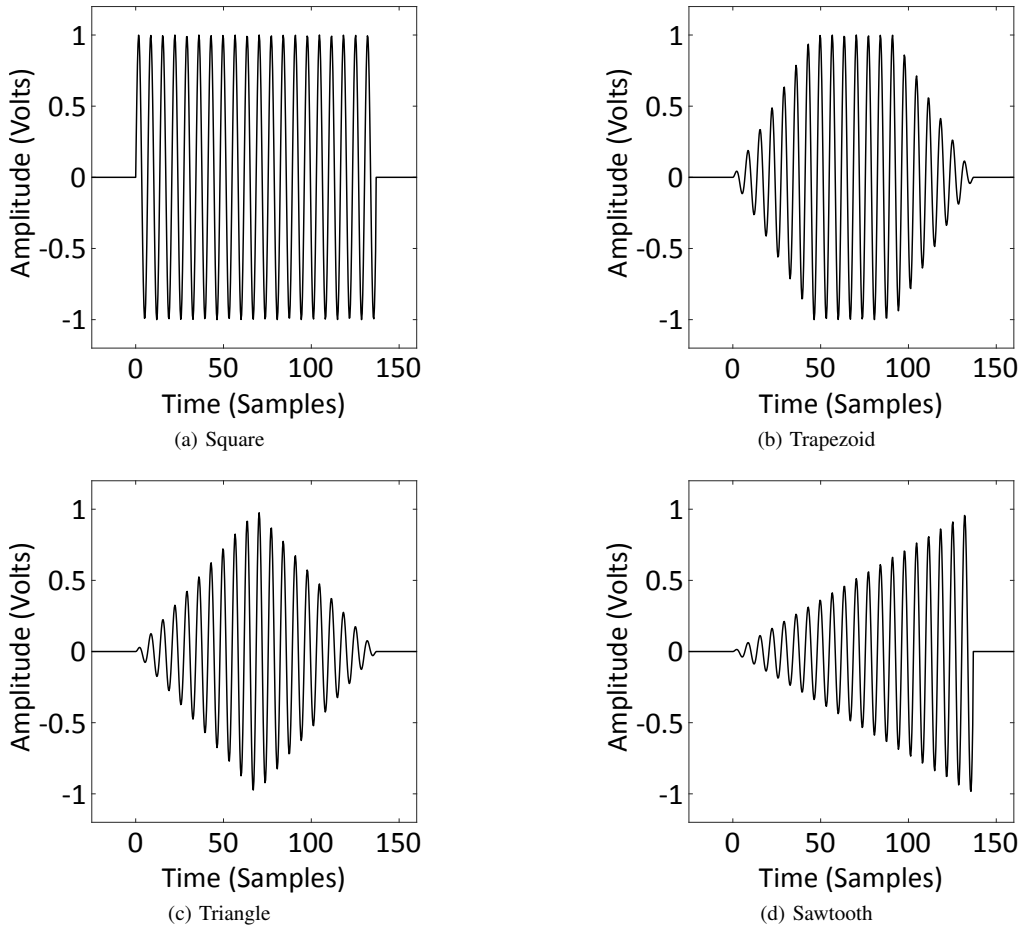

(a) Square (b) Trapezoid

(c) Triangle (d) Sawtooth

Fig. 6. The different output signals used in the experiment

In the blocks with more than one signal, as shown in Fig. 7b and 7d, the LOS signal always has a lower residual than that of the NLOS signals, which is as expected. Also, the residuals of the NLOS signals increase over time before converging to some value $r \gg 0$ whereas the residual for the LOS signal degreases gradually. Although the residual for the LOS signal in multi-signal blocks does not converge as close to zero as in the blocks with only one signal, it ends up far closer to zero than the residuals of NLOS signals.

Fig. 8a and 8b show the convergence of the parameters estimated from the same data demonstrating the difference between the algorithm running with and without the fast convergence weight update. In Fig. 8a the parameters $\hat{x}, \hat{y}, \hat{z}$ do converge and approach the true values in nearly 400 iterations. The result in 8b shows a vast improvement, convergence is achieved in 15 to 20 iterations. This result is consistent throughout the experimental data, all examples with successful classifications converge in less than 20 iterations.

The probability distributions used to calculate the probability in the Bayesian step were a pair of Gaussian distributions. These have worked very well during the tests, given that their standard deviations were calculated from a very limited quantity of data. Other distributions may outperform the Gaussian, but these have not been considered here. The role of the distribution is to give a very rough estimate for the regression step to refine. The regression step is where the bulk of the classification work is handled and as a result this allows a slightly relaxed approach to choosing these distributions.

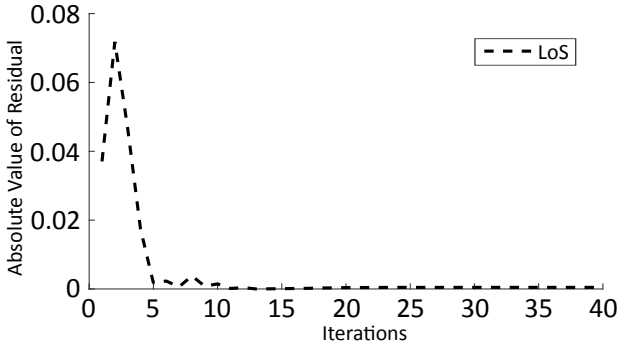

(a) Block 1 Residuals

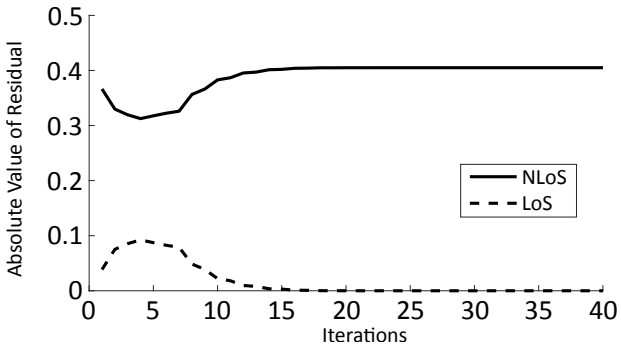

(b) Block 2 Residuals

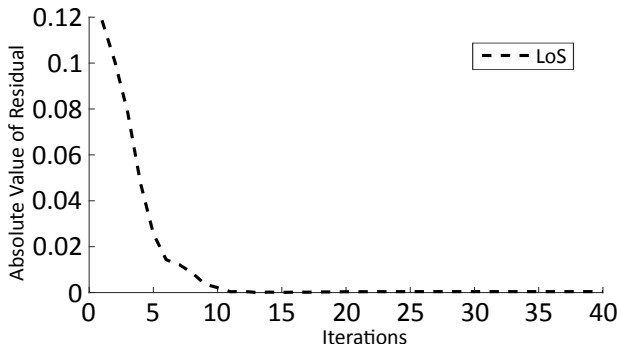

(c) Block 3 Residuals

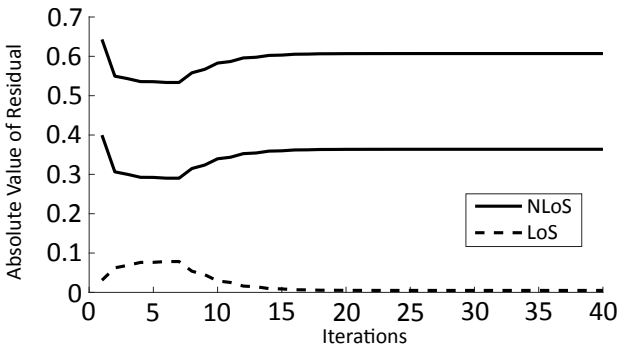

(d) Block 4 Residuals

Fig. 7. Residuals by block from a single regression

B. NLOS Classification Accuracy

Tables II and III show the NLOS classification results without and with acoustic padding respectively. As shown in Table 2, the percentage of correctly classified NLOS signals over the entire dataset exceeded 96% in case of triangle and sawtooth

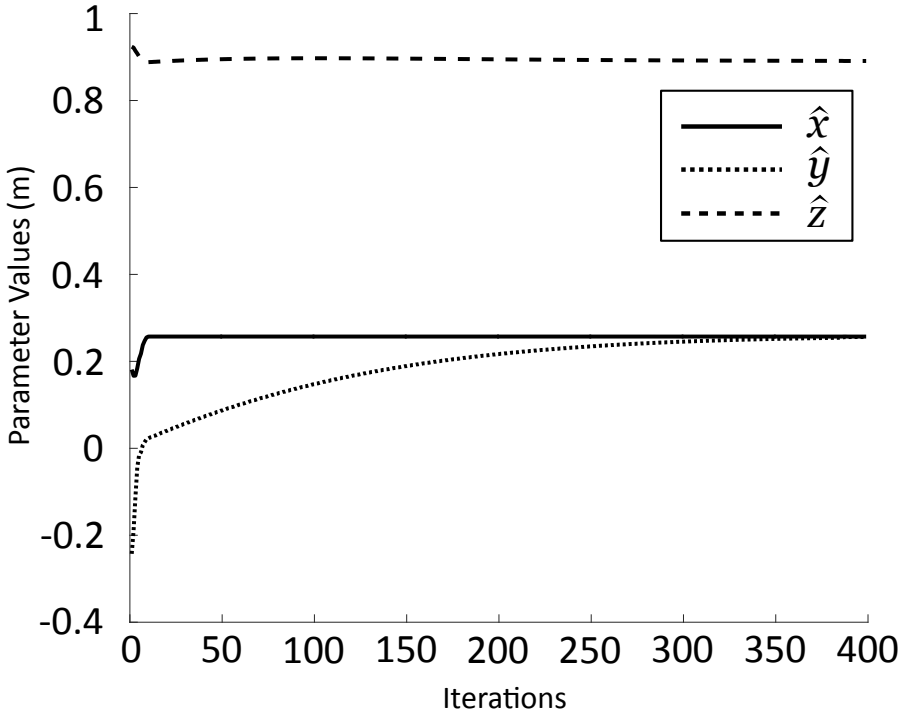

(a) Regular Convergence of Parameters $\hat{x}, \hat{y}, \hat{z}$ (0 - 400 Iterations)

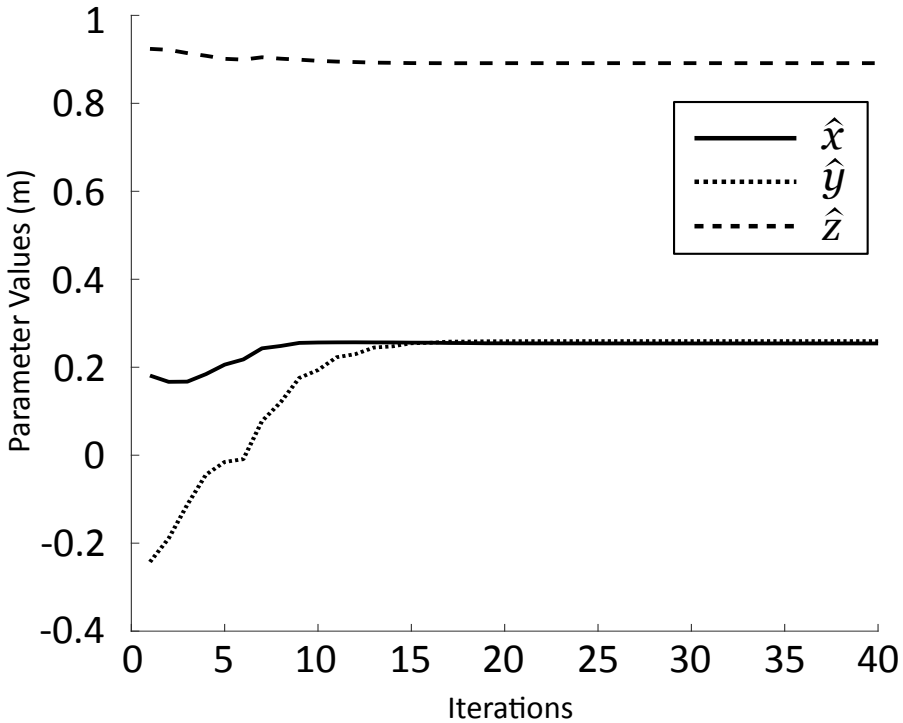

(b) Fast Convergence of Parameters $\hat{x}, \hat{y}, \hat{z}$ (0 - 40 Iterations)

Fig. 8. Comparison of parameter convergence

envelope signals and 99% in case of square, trapezoid shaped signals. These measurements were performed under severe multipath conditions with multiple reflections registered in each localisation frame and demonstrate the robustness of the proposed algorithm. When the acoustic padding was used to reduce the number of reflections the classification accuracy increased to 100%.

TABLE II
NLoS Classification Results Without Acoustic Padding

Envelope Type	Correct NLoS Classification	Incorrect Classification	% Correctly Classified
Square	4543	22	99.5
Trapezoid	4928	34	99.3
Triangle	5178	132	97.5
Sawtooth	5072	160	96.9

TABLE III
NLoS Classification Results With Acoustic Padding

Envelope Type	Correct NLoS Classification	Incorrect Classification	% Correctly Classified
Square	297	0	100
Trapezoid	407	0	100
Triangle	419	0	100
Sawtooth	414	0	100

C. Localisation accuracy

Tables IV and V show the accuracy of the 1D distances and 3D positions calculated by the algorithm. Firstly, the accuracy of the system with acoustic padding is better than that of the system without it. From the standard deviations and the minimum and maximum values it can be seen that the spread of errors is wider in the data from the unpadded experiments. The accuracy of the range measurement could be further improved by fine tuning the transmitted signal characteristics and selecting more refined TOF estimation method [3]-[5]. However, even with the existing errors in the 1D range measurements and despite the simplicity of the TOF estimation, RoBCUL algorithm has demonstrated robustness not only in finding the solution for the receiver position but also correctly rejecting reflections in the great majority of cases, as shown in Tables II and III.

Fig. 9 shows the 1D range measurement errors for different distances between the transmitter and the receiver planes over the entire dataset for all of the signals combined.

TABLE IV
Measurement Error in Millimetres From all Experiments With Acoustic Padding

Envelope Type	1D/3D	Mean	Std. Dev.	Max.	Min.
Square	1D	0.61	6.49	21.44	-19.19
Square	3D	2.92	7.33	27.66	-10.03
Trapezoid	1D	0.67	6.19	21.59	-16.14
Trapezoid	3D	5.41	4.19	22.22	0.06
Triangle	1D	0.38	6.35	21.58	-19.44
Triangle	3D	4.91	3.77	22.00	0.01
Sawtooth	1D	9.23	5.67	27.95	-10.74
Sawtooth	3D	11.85	8.76	39.25	-13.57

TABLE V
MEASUREMENT ERROR IN MILLIMETRES FROM ALL EXPERIMENTS WITHOUT ACOUSTIC PADDING

Envelope Type	1D/3D	Mean	Std. Dev.	Max.	Min.
Square	1D	-2.32	13.81	68.35	-37.95
Square	3D	-2.68	8.84	38.38	-10.03
Trapezoid	1D	-0.69	13.73	68.29	-46.53
Trapezoid	3D	8.68	8.83	48.37	0.03
Triangle	1D	-0.57	16.29	143.39	-47.62
Triangle	3D	8.68	8.84	48.38	0.03
Sawtooth	1D	8.33	14.7	170.38	-34.02
Sawtooth	3D	9.14	11.81	55.75	-20.49

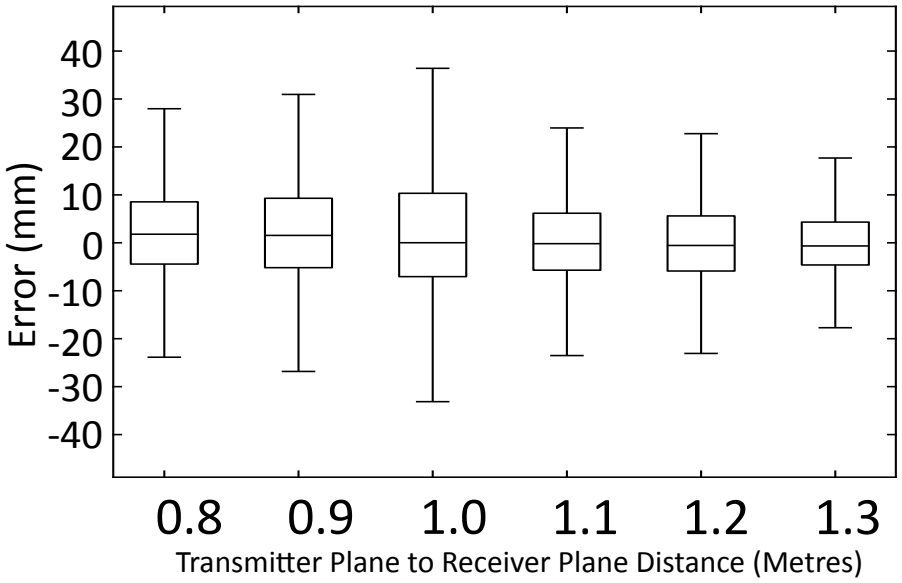

(a) Range Measurement Error without Acoustic Padding

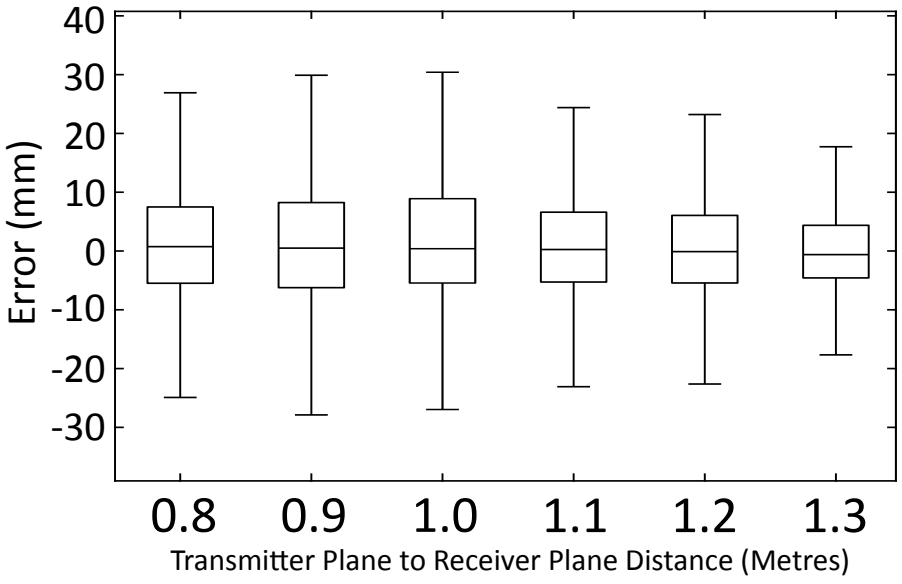

(b) Range Measurement Error with Acoustic Padding

Fig. 9. One Dimensional Range Measurement Errors

The results have shown that range measurement error does not significantly change with the distance. The range of 80 to 130 cm was chosen due to the constraints of the physical setup and the specific application requirements as discussed in [12]. However, it is important to emphasize that the maximum location range of the proposed method is not limited to 130 cm. Although, the range measurement error is usually worse with distance due to attenuation of the ultrasonic signals and increased level of noise, there is no inherent range limit in the RoBCUL algorithm because it was designed to estimate whether a particular signal is LOS or NLOS from the available information. In fact, in a larger environment, that has reflective surfaces further apart, the RoBCUL should be able to classify multipath signals more easily because the amplitudes of the NLOS signals will be relatively more attenuated than LOS due to a longer travel distance.

V. Conclusion

A novel robust and computationally efficient algorithm for rejecting reflections in ultrasonic localisation systems has been developed and presented. The RoBCUL is based on a probabilistic estimate fed into an IRLS regression. The general structure of the algorithm consists of two main parts: first, Bayesian probability assignment for the LOS and NLOS signals and second, adaptive IRLS classification using a combination of probability based on amplitude and regression residual.

The RoBCUL algorithm robustness in classification and rejection of NLOS has been tested on a large quantity of experimental data containing many specular reflections. The results have shown the algorithm performance in correctly classifying and rejecting over 96% of NLOS signals under severe multipath conditions not normally found in the previously published research. The method was also capable of performing this task at significantly lower computational cost than similar technique described in the literature [10].

Although, this method can be applied in many localisation systems that utilise time division multiplexing, the specific application which this technique is aimed at is a new device for anthropometric measurements in which robust rejection of reflected signals is an essential component [12]. Such measurements are important for routine postural assessments of individuals with severe neuromusculoskeletal and postural conditions resulting in limited body movement. The new measurement device that is currently being developed needs to cover points in a volume of approximately 50 cm^3 in order to capture 3D positions of various anatomical landmarks.

Further work is needed to improve the accuracy of the TOF estimation, mitigate the effect of complete signal blockage and refine the signal processing scheme.

References

[1] G. Kaniak and H. Schweinzer, "A 3d airborne ultrasound sensor for high-precision location data estimation and conjunction," *Conference Record - IEEE Instrumentation and Measurement Technology Conference*, pp. 842–847, 2008.

[2] M. Parrilla, J. Anaya, and C. Fritsch, "Digital signal processing techniques for high accuracy ultrasonic range measurements," *IEEE Transactions on Instrumentation and Measurement*, vol. 40, no. 4, pp. 759–763, 1991.

[3] L. Angrisani and R. Schiano Lo Moriello, "Estimating ultrasonic time-of-flight through quadrature demodulation," *IEEE Transactions on Instrumentation and Measurement*, vol. 55, no. 1, pp. 54–62, 2006.

[4] R. Raya, A. Frizera, R. Ceres, L. Calderón, and E. Rocon, "Design and evaluation of a fast model-based algorithm for ultrasonic range measurements," *Sensors and Actuators, A: Physical*, vol. 148, no. 1, pp. 335–341, 2008.

[5] S. Jiang, C. Yang, R. Huang, C. Fang, and T. Yeh, "An Innovative Ultrasonic Time-of-Flight Measurement Method Using Peak Time Sequences of Different Frequencies: Part I," *IEEE Transactions on Instrumentation and Measurement*, vol. 60, no. 3, pp. 735–644, 2011.

[6] P. Lazik and O. Shih, "ALPS : A Bluetooth and Ultrasound Platform for Mapping and Localization," *ACM SenSys*, pp. 73–84, 2015.

[7] N. B. Priyantha, A. Chakraborty, and H. Balakrishnan, "The Cricket Location-support System," *Proceedings of the 6th Annual International Conference on Mobile Computing and Networking*, no. August, pp. 32–43, 2000.

[8] T. Aguilera, F. J. lvarez, D. Gualda, J. M. Villadangos, . Hernndez, and J. Urea, "Multipath compensation algorithm for tdma-based ultrasonic local positioning systems," *IEEE Transactions on Instrumentation and Measurement*, vol. PP, no. 99, pp. 1–8, 2018.

[9] J. C. Prieto, C. Croux, and A. R. Jiménez, "RoPEUS: A new robust algorithm for static positioning in ultrasonic systems," *Sensors*, vol. 9, no. 6, pp. 4211–4229, 2009.

[10] T. Qiao and H. Liu, "Improved Least Median of Squares Localization for Non-Line-of-Sight Mitigation," *IEEE Communication Letters*, vol. 18, no. 8, pp. 1451–1454, 2014.

[11] J. Khodjaev, S. Tedesco, and B. O. Flynn, "Improved NLOS Error Mitigation Based on LTS Algorithm," *Progress In Electromagnetics Research Letters*, vol. 58, no. October 2015, pp. 133–139, 2016.

[12] J. Kulon, M. Voysey, A. Partlow, P. Rogers, and C. Gibson, "Development of a System for Anatomical Landmarks Localisation Using Ultrasonic Signals," *IEEE International Symposium on Medical Measurements and Applications (MeMeA), Benevento*, pp. 369–374, 2016.

[13] N. Friedman, D. Geiger, and M. Goldszmit, "Bayesian Network Classifiers," *Machine Learning*, vol. 29, pp. 131–163, 1997.

[14] W. T. Freeman and D. H. Brainard, "Bayesian decision theory, the maximum local mass estimate, and color constancy," *Proceedings of IEEE International Conference on Computer Vision*, pp. 210–217, Jun 1995.

[15] Y. Ephraim, "A Bayesian Estimation Approach for Speech Enhancement Using Hidden Markov Models," *IEEE Transactions on Signal Processing*, vol. 40, no. 4, 1992.

[16] D. W. Marquardt, "An Algorithm for Least-Squares Estimation of Nonlinear Parameters," *Journal of the Society for Industrial and Applied Mathematics*, vol. 11, no. 2, pp. 431–441, 1963.